Pulsed Eddy Current Detection of Loose Parts in Steam Generators

Dylan P. Johnston, Jeremy A. Buck, Peter Ross Underhill, Jordan Morelli and Thomas W. Krause

***Abstract* – Flow induced vibration of loose parts located on steam generator (SG) tube sheets can result in SG tube damage and eventual loss of SG efficiency. Regular inspection of SG tubes at support structures can help extend SG life by detecting and monitoring flaws as well as identifying accumulation of loose parts. Application of conventional eddy current technologies in this case however, is limited when magnetite fouling is present or when loose parts are resting directly on the SG tube sheet. Pulsed eddy current (PEC) combined with a modified principal components analysis (MPCA) was investigated as a method of detecting and identifying a variety of loose part materials in close proximity to 16 mm outer diameter Alloy-800 SG tubes and surrounding steel support structures. Loose parts were found to be detectable for varying axial positions along the SG tube and when in contact with the tube sheet. When offset radially from the SG tube, 1.6 mm diameter carbon steel parts with a strong magnetic component allowed detection up to 3.2 mm away, while non-ferromagnetic stainless steel parts of the same size could only be detected up to 1.5 mm away. Signal variation in the presence of loose parts was attributed to differences in amplitude of transient response and in relaxation times for diffusion of transient magnetic fields through the various materials. The ability to accurately detect and identify loose parts located in close proximity to SG tubes establishes PEC combined with MPCA as a potential candidate for SG inspection.**

***Index Terms* – Alloy 800, non-destructive testing, principal components analysis, pulsed eddy current, steam generator tube, loose parts.**

This work was supported by University Network of Excellence in Nuclear Engineering (UNENE) and the Natural Sciences and Engineering Research Council of Canada (NSERC)

D. P. Johnston is with the Department of Physics, Queens University, Kingston ON K7L3N6, Canada, (email: mail.dylan.13@gmail.com)

J. A. Buck was with the Department of Physics, Royal Military College of Canada, Kingston ON K7K7B4, Canada, (email: buck.j4@gmail.com) and is now with Canadian Nuclear Laboratories, Chalk River Laboratories, Chalk River, ON K0J1J0 (email: jeremy.buck@cnl.ca)

P.R. Underhill is with the Department of Physics, Royal Military College of Canada, Kingston ON K7K7B4, Canada, (e-mail: ross.underhill@rmc.ca)

J. Morelli is with the Department of Physics, Engineering Physics and Astronomy, Queen's University, Kingston ON K7L3N6, Canada, (email: morelli@physics.queensu.ca)

T.W. Krause is with the Department of Physics, Royal Military College of Canada, Kingston ON K7K7B4, Canada, (e-mail: thomas.krause@rmc.ca)

I. INTRODUCTION

Steam generators (SGs) in nuclear reactors undergo regular inspections in order to monitor the condition of SG tubes, while providing evidence of their continued safe operation [1]. [2].

A variety of degradation modes can be present within SGs, including stress corrosion cracking and fretting wear on SG tubing, support structure degradation and corrosion, and the accumulation of magnetite sludge on the SG support structures [1]. Loose parts, which may appear in SGs after maintenance has been performed or detach from support structures due to corrosion, accumulate primarily on top of the tube sheet [3]. Loose parts that are in physical contact with SG tubes and exposed to flow, can vibrate and cause fretting wear. This in turn produces more metallic debris and, eventually, compromises the integrity of SG tube structures, if not removed [2] [4].

Detection of these loose parts is imperative for maintaining plant efficiency, since SG tubes are 'plugged' once 40% through-wall frets are detected [4]. Currently, ET is the primary non-destructive testing method used to detect loose parts that lie within 3 millimetres of non-magnetic Alloy 800 SG tubes [2] and not in contact with the ferromagnetic tube sheet. However, the inspection performance of ET is reduced in the presence of magnetite fouling [2], and when multiple modes of degradation are present [2]. Additionally, ET encounters difficulties in detecting loose parts in the presence of ferromagnetic materials such as tube sheets or other support structures within the SG [2]. The absence of available techniques and challenges associated with current ET techniques at the ferromagnetic tube sheet, motivates the development of other inspection technologies for the detection of loose parts.

Pulsed Eddy Current testing (PEC) is an emerging non-destructive testing technique that has been developed for the inspection of nuclear and aerospace structures [5] [6] [7] [8]. Instead of the continuous sinusoidal signal utilized by ET, PEC employs a square wave voltage pulse to induce eddy currents in conductive media. Transient voltage responses induced in pick-up coils by these eddy currents can be considered as consisting of a distribution of discrete frequencies. Thus, PEC has a spectrum of frequencies available for interaction with the inspected component, as opposed to the few discrete frequencies that are generated by the ET drive signal [9]. In addition, the approach to direct current (DC) excitation in the pulse provides partial magnetization of

ferromagnetic materials, which enhances the pick-up coil response as opposed to hindering it, as is the case in conventional ET [10].

Principal Components Analysis (PCA) of PEC has shown an improved ability to classify defects over that of conventional techniques [11]. In this work, PEC pick-up coil responses have been analyzed using Modified Principal Components Analysis (MPCA) [12]. Like PCA, MPCA reconstructs the signal using orthogonal basis vectors and associated scores, thereby reducing the dimensionality of the data. However, MPCA does not use subtraction of the average response, as used in conventional PCA. This is equivalent to a minimization of sum square residuals interpretation as formulated in Ref. [12], instead of a variance minimization, as used in conventional PCA [13]. When combined with PEC, MPCA has been found to be a robust analysis technique for measurement of tube-to-support gaps and SG tube fretting [14] [15]. Some of its ability to separate features has been attributed to differences in relaxation times for diffusion of transient fields through the tube compared with diffusion into the ferromagnetic support structure [14] [8]. In aerospace NDT, PEC was able to detect stress-corrosion cracking defects, which were undetectable using conventional eddy current due to large lift-off distance [5], [16]. In nuclear reactor non-destructive testing, artificial neural networks, applied to PEC signal analysis, showed that simultaneous extraction of tube position in two dimensions, tube wall loss (fretting wear), and support structure corrosion could be achieved [7]. PEC has also been used to characterize low-energy impacts and inserted defects in carbon fiber reinforced polymer laminates [17] and corrosion of mild steels [18]. Chen et. al. [19] have applied the Hilbert transform for feature extraction in order to attain robust and rapid identification of different defects.

This report examines PEC response to various types and sizes of metal loose parts. Detection of loose parts is examined for orientations parallel and perpendicular to the SG tube at or near the tube sheet. The experimental setup and a description of the measurement technique are presented in *Section II*. *Section III* presents results and discussion of using MPCA and cluster analysis of PEC signals for detection of loose parts, and *Section IV* provides a summary of this work.

II. EXPERIMENT

A. *Apparatus*

Six Alloy-800 tubes, 457 mm in length, and one Alloy-800 tube, 305 mm in length, were used to recreate the SG tube structure for this investigation. Each tube had nominal wall thickness of 1.2 mm and outer diameter of 15.9 mm. A simulated tube sheet support plate of thickness 25 mm was used to hold the Alloy-800 tubes in place as shown in Figure 1. The 305 mm Alloy-800 tube was installed as manufactured, while the other six tubes all possessed various degrees of fretting wear. The unfretted tube was used for data acquisition as it represents nominal tube condition. Figure 1 shows the SG configuration with radial (away from the SG tube) and axial (away from the tubesheet) offset directions as indicated.

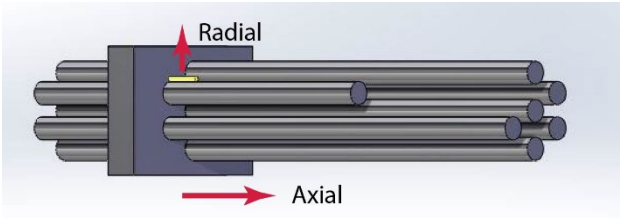

Figure 1: Steam generator tube structure showing radial and axial offset directions with loose part (yellow) in parallel orientation.

B. *Loose Parts*

The loose parts used in this investigation are listed in Table 1 along with their relevant dimensions and conductivity values. The conductivity values were taken from [20] [21] [22].

Four 3.2 mm thick plastic shims were used to offset loose parts away from the SG tube, defined as the radial direction (see Figure 1). Two magnetite collars, of thickness 2.5 mm and 3.2 mm, were used to offset loose parts in the same way, simulating magnetite sludge surrounding the SG tube (see Figure 2). Minimum magnetite offset was limited to 2.5 mm as this was the smallest magnetite thickness that could be mechanically maintained. Both collars had a measured relative magnetic permeability of 1.9, typical of that found around SG tubes [23]. Loose parts were oriented with their axis either parallel or perpendicular to the SG tube.

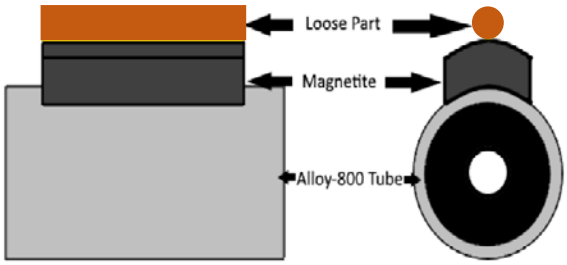

Figure 2: Steam Generator tube with loose part in parallel orientation, offset by a piece of magnetite.

C. *Probe*

The probe used in this investigation, described in detail elsewhere [14] [24], consisted of a drive coil and eight pick-up coils: four located in front (front array) and four located behind (back array) the drive coil. These coils are spaced azimuthally at 90-degree intervals. The probe body with dimensions is shown in Figure 3. Pickup coils that were 180° apart were paired for analysis. Front array signals were used in this analysis [12] so the drive coil was closer to the tube sheet than the pickups. Shielded twisted pair wire carried the signals from the pickup coils to an amplification circuit.

TABLE 1: LOOSE PARTS INCLUDED IN INVESTIGATION

Material	Label	Diameter (mm)	Length (mm)	Conductivity[2] (MS/m) (T=20℃)
Brass	1/8”	3.2	25.9	14.3
	1/4”	6.3	26.7	
	1/2”	12.7	25.9	
	1”	25.4	24.0	
Carbon Steel	1/16”	1.6	27.0	5.9
	1/8”	3.2	25.0	
	1/4”	6.3	25.9	
	1/2”	12.7	25.4	
	1”	25.4	25.6	
Copper	1/8”	3.2	26.3	58.1
Lead[1]	1/10”	2.3	41.8	4.9
Stainless Steel (300 Series)	1/16”	1.6	26.2	1.4
	1/8”	3.2	25.3	
	1/4”	6.3	26.1	
	1/2”	12.7	25.7	
	1”	25.4	25.9	
Tin	1/8”	3.3	29.3	7.9

[1]Lead part was a bar with square cross-section –equivalent area circular diameter given.
[2]Conductivity values taken from [20] [21] [22].

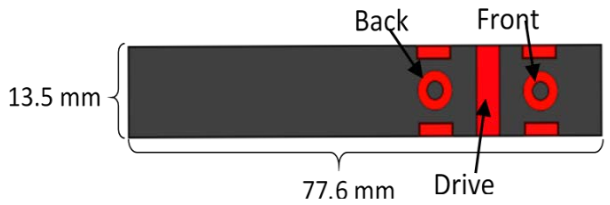

Figure 3: PEC Probe Schematic showing pickup coil arrays behind (back and in front (front) of the drive coil

A timed LabVIEW program was used to generate excitation pulses and collect voltage responses from the pickup coil array. The signals from each pickup coil were individually amplified with a gain of 100 before being digitized at 1MHz using a 16-bit resolution NI6356 USB DAQ. The DAQ was connected to a laptop computer that was used to save the data and perform MPCA on the acquired data. The NI6356 USB DAQ was also used to generate the excitation pulse, which was then buffered to provide sufficient current for the drive coil. The pulse was generated by the USB DAQ at 1000 Hz and 50% duty cycle, and voltage driven amplitude of 1.5 V, corresponding to peak current of 170 mA for a 9.0 Ω drive coil resistance.

D. Data Gathering

The probe was initially inserted into the SG tube so that the drive coil was 100 mm from the edge of the tube sheet. Measurements were then taken at 2 mm intervals within the Alloy-800 SG tube as the probe was axially translated a distance of 130 mm through the SG tube, for a total of 65 data points. The loose parts were aligned with the probe’s pickup coils, in order to maximize pickup coil response. Temperature was recorded for each data acquisition. The principal components were constructed from trials involving the parts listed in Table 1 oriented both parallel and perpendicular to the SG tube, for a variety of axial and radial offset positions.

III. RESULTS & DISCUSSION

A. Probe Response

The transient responses of the probe in the presence of just the SG tube (null trial), a 3.2 mm diameter carbon steel part, and a 3.2 mm diameter copper part, are shown in Figure 4. Variations in the transient response of the probe are attributed to differences in degree of electromagnetic interaction with the probe and characteristic diffusion times for different materials. The absolute signals from opposite coils were combined symmetrically into a single vector for MPCA analysis [12]. An example of MPCA signal decomposition for as-acquired data to resultant eigenvectors is shown in Ref. [5].

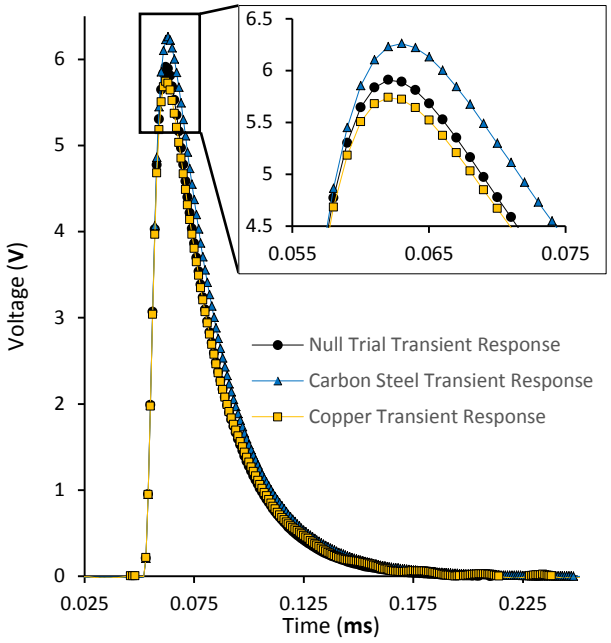

Figure 4: Transient voltage response of a pick-up coil in the presence of an Alloy-800 tube, an Alloy-800 tube and a 3.2 mm diameter carbon steel part, and an Alloy-800 tube and a 3.2 mm copper part. Neither part possessed a radial offset

B. MPCA

Data sets were formed for each loose part material and the null case from the individual measurements as the probe was translated along the steam generator tube towards the tube sheet. One data set for each loose part material was then combined into a global data set that was used to generate principal components using MPCA. In order for the MPCA to be accurate, it was important that this data set span the range of all expected probe responses. The MPCA procedure produces principal

components (eigenvectors), which are common to all the data and scores that contain the specific information about each signal. The principal components can be used to produce scores for data not in the original MPCA, which are accurate provided the eigenvectors span the space of the signals. It was found that, using the first four principal components, the measured signal could be reproduced with an average mean square error of less than 0.1% for all the data. Higher order principal components were found to contain noise and were, therefore, not included. Half of each eigenvector, corresponding to the coil closest to the spare part is shown in Figure 5. The other half was either identical (symmetric) or inverted (antisymmetric).

The first principal component (V1), which was symmetric between the two coils, approximately accounts for the average response of the data and thus, resembles the raw transient signal shown in Figure 4. The scores associated with the first principal component were found to be at least an order of magnitude larger than other component scores. The second principal component (V2, which was also symmetric) can be seen peaking earlier in time than the first principal component, and possesses a second peak of opposite sign. Hence, depending on the sign of the associated score, it represents the shift of signal to earlier or later times and a change in the relaxation time of the probe. Hence, it might be expected to be very sensitive to the tube sheet amongst other effects. The third principal component (V3) has a shape similar to the first principal component (V1), but is antisymmetric and therefore, represents the shifting of intensity from the coil closest to the loose object to its partner coil or vice versa. Hence, scores associated with this eigenvector might be expected to be very sensitive to the presence of loose parts.

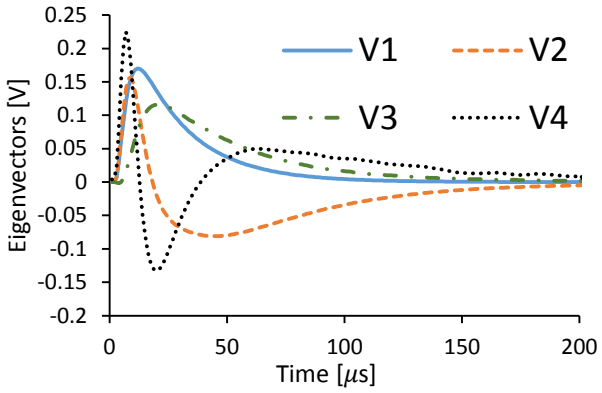

Figure 5: Eigenvectors constructed by performing MPCA on a global data set.

The most direct method of determining the presence of loose parts is to compare scores obtained when the part was present to those of a null trial (no loose part) as a function of axial displacement. In the absence of a loose part, scores were observed to remain unchanged between data sets. Therefore, if a score variation was observed, it could be inferred that a loose part was present at that axial position on the SG tube. This was observed to be the case for carbon steel loose parts as shown in Figure 6 for scores associated with V3, for a 1.6 mm Dia. part in contact with the steam generator tube and the tube sheet. In this case, the orientation of the loose part can also be inferred from the extent of the deviation in scores as the probe is translated down the tube. In addition, the score deviation is also less for the perpendicular alignment as the orientation of the loose part reduces its interaction with the probe even when they are directly aligned.

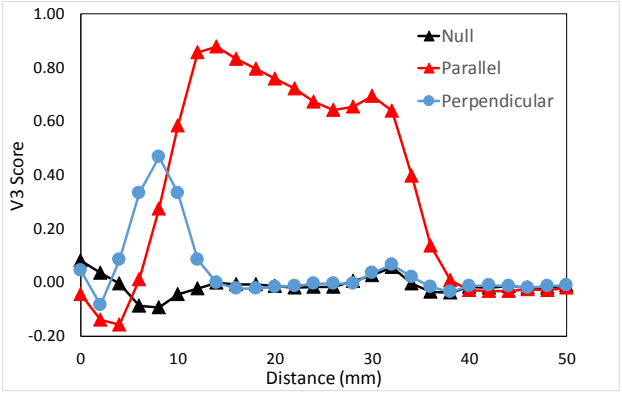

Figure 6: 1.6 mm diameter carbon steel loose part in both parallel and perpendicular orientations with no radial or axial offset compared with null trial. Distance is distance from the tube sheet.

While the direct use of PCA scores worked well for carbon steel in direct contact with the steam generator tube, in general, the deviations in any one score were too small to provide reliable evidence of the loose part for other materials and when the loose part was not in contact with the steam generator tube. A more sophisticated approach that combines the variation in multiple scores is required to overcome this limitation. A vast variety of techniques, including neural networks [7], SVM machines [25] and cluster analysis [26], to mention a few, have been used by various authors for this purpose. In this paper, a cluster analysis approach was used. The concept behind this is that measurements from loose-part free tubes should be very similar and form a cluster. The presence of a loose part should shift the measurement away from this cluster.

C. Cluster Analysis

The spare parts were detected using a cluster analysis approach based on the Mahalanobis distance [13] [26]. In order to use this approach a covariance matrix and mean vector for the null case needed to be constructed. However, as would be expected, the mean response and therefore, the null, of the probe changed as the probe approached the tube sheet. This is shown in Figure 7 for Score 4. Similar curves were obtained for each of the other three scores. Dealing with just 4 scores, rather than the entire data set of 120 points, as required for the equivalent process in conventional PCA, simplifies and expedites the analysis. In order to deal with this, the signal response for each score was plotted as a function

of position for the null case (see Figure 7) and an exponential curve was fit to the data. This curve was then used to define the mean value at each location and the difference between the curve and the measured data was used to generate the covariance matrix for the null case.

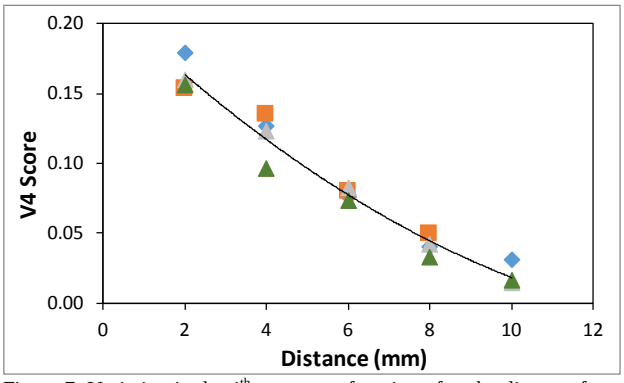

Figure 7: Variation in the 4th score as a function of probe distance from the tube sheet. Different colours represent different runs.

It can be shown that the Mahalanobis distance for the null case is distributed as a chi-square with p degrees of freedom, where p is equal to the number of scores used in forming the Mahalanobis distance [27]. This makes it possible to define a critical size based on the false call rate that can be tolerated. In the current case, only scores for vectors 2 to 4 were used to construct the Mahalanobis distance, so a 95% confidence interval is 2.80. Using this cut-off will generate a false call 5% of the time. In fact, the situation is a little more complicated. In order to "find" a loose part, the Mahalanobis distances for each of the last 5 points in the scan (shown in Figure 7) were computed. A hit on any one of those points would be taken as indicating the presence of a loose part. Assuming that variations in the measurements are independent for the null case, in order to achieve a 5% false call rate overall, one needs to have 1.0% chance of a false call on any one of the measurements. This corresponds to a critical Mahalanobis distance of 3.36.

The second, third, and fourth principal component scores were most commonly plotted for this type of analysis, since the more difficult to detect parts demonstrated the least variation in the first principal component score.

Cluster analysis was only applied to parts with diameter of 3.2 mm or less, as parts larger than this were found to be quite readily detectable under the conditions tested. In terms of composition, copper was the most detectable non-ferromagnetic material. Figure 9 shows that materials with higher conductivity values also exhibited larger score variations. This result is attributed to the dependence of transient response variation on the strength of the electromagnetic interaction and on differences in characteristic diffusion times. The most difficult to detect material, stainless steel, for example, possessed the lowest conductivity of the materials tested. Ferromagnetic materials, such as carbon steel, showed variation in the opposite direction of non-ferromagnetic materials, possibly reflecting the response of the cluster analysis to magnetization effects.

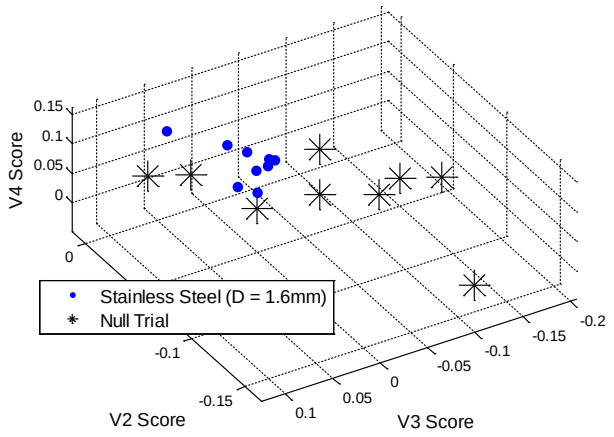

Figure 8: 1.6 mm stainless steel loose part oriented parallel to the SG tube with no axial or radial offset.

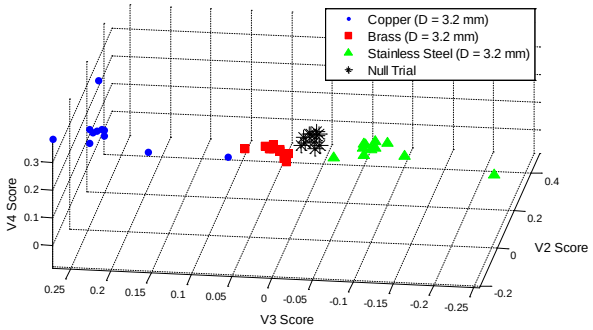

Figure 9: 3.2 mm diameter loose parts of varying composition with no radial or axial offset.

Loose parts that were larger, had a greater electromagnetic interaction with the pickup coil and possessed a longer relaxation time associated with their larger diameter and corresponding characteristic length [28] [29]. It is presumed that both of these factors will affect the score outcome. Detectability was also found to decrease rapidly when parts were offset radially from the SG tube, reducing the electromagnetic interaction, as seen in Figure 11 . Both Figure 10 and Figure 11 demonstrate the effect that differences in the part size and radial offset position have on detectability, respectively.

The score variation observed from a loose part that was offset axially from the tube sheet was found to be of the same, or of slightly lower magnitude compared to that of a loose part in contact with the tube sheet. This effect is likely caused by the voltage amplification due to local magnetization of the ferromagnetic tube sheet, resulting in an effect that is opposite that observed in conventional eddy current [2].

Table 2 compares the maximum radial distance that a part could be detected, both in the presence and absence of magnetite. Note that measured minimum distances are a function of available spacer thickness. In all of these

cases, signals were sufficiently small that cluster analysis approach had to be used to identify the sample. A detectable offset less than 2.5 mm means that the sample could not be detected in the presence of magnetite collars that were available. In most cases, when magnetite was present, there was a reduction in the radial distance at which the sample could be detected. The two cases where no reduction was seen probably resulted from the step size for the no-magnetite case being too large and may well have shown an effect with smaller step sizes.

Cluster analysis, performed on MPCA scores obtained from PEC signals, has demonstrated the potential for detection and classification of external loose parts from within nonmagnetic SG tubes and on top of ferromagnetic support plate. This type of analysis may have other potential applications such as, for example, using identification of outliers for the detection of second layer cracks in aerospace wing structures [26].

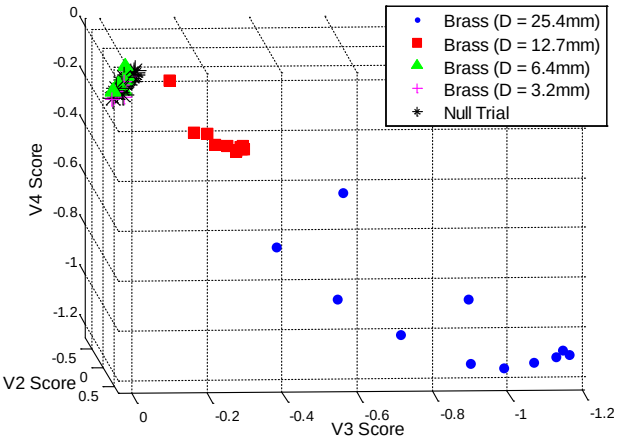

Figure 10: Brass loose parts ranging from 3.2 mm in diameter to 25.4 mm in diameter with no radial or axial offset.

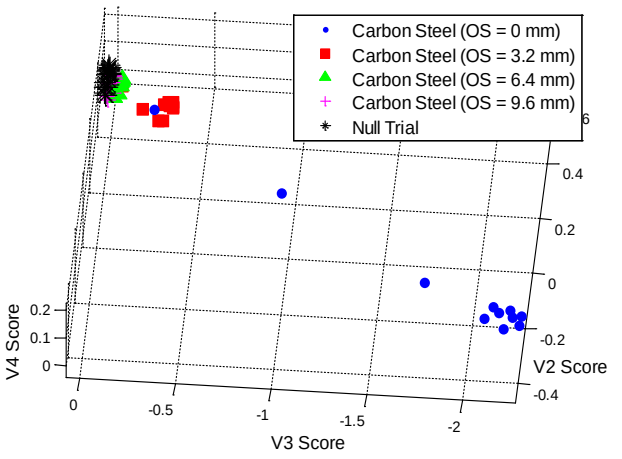

Figure 11: 3.2 mm diameter carbon steel loose part in contact with the tube sheet at various radial offsets (OS). Score variation magnitude drops off quickly with radial offset.

TABLE 2: MAXIMUM RADIAL DISTANCE AT WHICH LOOSE PARTS IN CONTACT WITH THE TUBE SHEET ARE DETECTABLE UNDER MAGNETITE AND NON-MAGNETITE CONDITIONS.

Loose Part (diameter)	Maximum radial offset detectable (mm)	Maximum radial offset detectable (magnetite) (mm)
Carbon Steel (3.2 mm)	9.6 mm	3.2 mm
Carbon Steel (1.6 mm)	3.2 mm	3.2 mm
Brass (3.2 mm)	3.2 mm	3.2 mm
Stainless Steel (3.2 mm)	3.2 mm	< 2.5 mm
Stainless Steel (1.6 mm)	1.5 mm	< 2.5 mm
Copper (3.2 mm)	3.2 mm	2.5 mm
Lead (2.3 mm)	0.5 mm	< 2.5 mm

IV. CONCLUSION

This work investigated the application of pulsed eddy current and modified principal components analysis as a method of detecting and identifying loose parts from within non-magnetic Alloy-800 SG tubes in proximity to ferromagnetic tube sheets, which were composed of carbon steel. Materials spanning a wide range of conductivities, representing potential loose part materials, were included in the investigation.

Loose parts were found to be detectable both in contact with the tube sheet and in the presence of magnetite. The detectability of the loose parts depended on their size, permeability, conductivity and radial distance from the SG tubes as would be expected. MPCA combined with cluster analysis was shown to be a robust analysis technique that extended the detectability to more challenging samples.

ACKNOWLEDGMENT

The first author would like to thank Vijay Babbar, and Brian Lepine at Canadian Nuclear Laboratories (CNL) for useful discussion.

REFERENCES

[1] D. R. Diercks, W. J. Shack and J. Muscara, "Overview of Steam Generator Tube Degradation and Integrity Issues," *Nuclear Engineering and Design*, vol. 194, no. 1, pp. 19-30, 1999.

[2] M. H. Attia, "Fretting Fatigue and Wear Damage of Structural Components in Nuclear Power Stations-Fitness for Service and Life Management Perspective," *Tribology International*, vol. 39, no. 10, pp. 1294-1304, 2006.

[3] B. L. Jarman, I. M. Grant, R. Garg and AECB, "Regulation of Ageing Steam Generators," in *Canadian Nuclear Society*, Toronto, 1998.

[4] K.-W. Ryu, C.-Y. Park, H.-N. Kim and H. Rhee, "Prediction of fretting wear depth for steam

generator tubes based on various types of fretting wear scars," *J. Nucl. Sci. Technol.*, vol. 47, no. 5, pp. 449-456, 2010.

[5] P. F. Horan, P. R. Underhill and T. W. Krause, "Real Time Pulsed Eddy Current Detection of Cracks in F/A-18 Inner Wing Spar Using Discriminant Seperation of Modified Principal Components Analysis Scores," *IEEE Sensors Journal,* vol. 14, no. 1, pp. 171-177, 2014.

[6] C. A. Stott, P. R. Underhill, V. K. Babbar and T. W. Krause, "Pulsed Eddy Current Detection of Cracks in Multilayer Aluminum Lap Joints," *IEEE Sensors Journal,* vol. 15, no. 2, pp. 956-962, February, 2015.

[7] J. A. Buck, P. R. Underhill, J. Morelli and T. W. Krause, "Simultaneous Multi-Parameter Measurement in Pulsed Eddy Current Steam Generator Data using Artificial Neural Networks," *IEEE Transactions on Instrumentation & Measurement,* vol. 65, no. 3, pp. 672-679, 2016.

[8] S. G. Mokros, P. R. Underhill, J. Morelli and T. W. Krause, "Pulsed eddy current inspection of wall loss in steam generator trefoil broach supports," *IEEE Sensors Journal,* vol. 17, no. 2, pp. 444-449, 2017.

[9] T. W. Krause, C. Mandache and J. H. V. Lefebvre, "Diffusion of Pulsed Eddy Currents in Thin Conducting Plates," *Review of Quantitative Nondestructive Evaluation,* vol. 27, pp. 368-375, 2008.

[10] D. R. Desjardins, G. Vallieres, P. P. Whalen and T. W. Krause, "Advances in Transient (Pulsed) Eddy Current for Inspection of Multi-Layer Aluminum Structures in the Presence of Ferrous Fasteners," *Review of Progress in Quantitative Nondestructive Evaluation,* vol. 31, no. 1, pp. 400-407, 2012.

[11] A. Sophian, G. Tian, D. Taylor and J. Rudlin, "A feature Extraction technique based on principal component analysis for pulsed eddy current NDT," *NDT&E International,* vol. 36, no. 1, pp. 37-41, 2003.

[12] P. F. Horan, P. R. Underhill and T. W. Krause, "Pulsed Eddy Current Detection of Cracks in F/A-18 Inner Wing Spar Without Wing Skin Removal Using Modified Principal Component Analysis," *NDT&E International,* vol. 55, no. 1, pp. 21-27, 2013.

[13] J. Lattin, D. Carroll and P. Green, in *Analyzing Multivariate Data,* Pacific Groove, CA, Brooks/Cole, 2003, pp. 83-123.

[14] J. A. Buck, P. R. Underhill, S. G. Mokros, J. Morelli, V. K. Babbar, B. Lepine, J. Renaud and T. W. Krause, "Pulsed Eddy Current Inspection of Support Structures in Steam Generators," *IEEE Sensors Journal,* vol. 15, no. 8, pp. 4305-4312, August 2015.

[15] S. Mokros, J. Buck, P. R. Underhill, J. Morelli and T. W. Krause, "Pulsed eddy current technology for steam generator tube support structure inspection," in *19th World Conference on Non-Destructive Testing,* Munich, Germany, 2016.

[16] Y. He, F. Luo, M. Pan, F. Weng, X. Hu, J. Gao and B. Liu, "Pulsed eddy current technique for defect detection in aircraft riveted structures," *NDT E International,* vol. 43, no. 2, pp. 176-181, 2010.

[17] Y. He, G. Tian, M. Pan and D. Chen, "Non-destructive testing of low-energy impact in CFRP laminates and interior defects in honeycomb sandwich using scanning pulsed eddy current," *Compos. Part B Eng.,* vol. 59, pp. 196-203, 2014.

[18] Y. He, G. Tian, H. Zhang, M. Alamin, A. Simm and P. Jackson, "Steel corrosion characterization using pulsed eddy current systems," *IEEE Sensors Journal,* vol. 12, no. 6, pp. 2113-2120, 2012.

[19] T. Chen, G. Y. Tian, A. Sophian and P. W. Que, "Feature extraction and selection for defect classification of pulsed eddy current NDT," *NDT & E International,* vol. 41, no. 66, pp. 467-476, 2008.

[20] V. S. Cecco, F. V. Drunen and F. L. Sharp, Eddy Current Testing: Manual on Eddy Current Method, Chalk River: Atomic Energy of Canada Limited, 1981.

[21] McMaster-Carr, "SS410 and CSA516 Material Properties," 2015. [Online]. Available: http://www.mcmaster.com/. [Accessed 13 July 2016].

[22] "Incoloy® alloy 800," 04 September 2004. [Online]. Available: www.specialmetals.com. [Accessed 13th July 2016].

[23] S. G. Mokros, "Pulsed Eddy Current Inspection of Broach Support Plates in Steam Generators," Queen's University, Kingston, 2015.

[24] T. W. Krause, V. K. Babbar and P. R. Underhill, "A Pulsed Eddy Current Probe for Inspection of Support Plates From Within Alloy-800 Steam Generator Tubes," *Review of Progress in Quantitative Nondestructive Evaluation,* vol. 33, pp. 1352-1358, 2014.

[25] Y. He, M. Pan, D. Chen and F. Luo, "PEC defect automated classification in aircraft multi-ply structure with interlayer gaps and lift-offs," *NDT and E Internaitonal,* vol. 53, pp. 39-46, 2013.

[26] D. M. Butt, P. R. Underhill and T. W. Krause,

"Examination of pulsed eddy current for inspection of second layer aircraft wing lap-joint structures using outlier detection methods," *CINDE Journal,* vol. 37, pp. 6-10, 2016.

[27] R. De Maesschalck, D. Jouan-Rimbaud and D. Massart, "Tutorial The Mahalanobis distance," *Chemometrics and intelligent laboratory systems,* vol. 50, pp. 1-18, 2000.

[28] H. C. Ohanian, "On the Approach to Electro- and Magento-static Equilibrium," *American Journal of Physics,* vol. 51, pp. 1020-1022, 1983.

[29] J. D. Jackson, "Quasi-Static Magnetic Fields in Conductorsl Eddy Currents; Magnetic Diffusion," in *Classical Electrodynamics 3rd Edition*, Hoboken, NJ, Wiley & Sons, 1999, pp. 219-238.

Dylan Johnston graduated from Queen's University in 2016 with a B.Sc.H in Astrophysics. Dylan's experimental research is on non-destructive inspection of steam generator tube support structures using pulsed eddy current, a project involving statistical techniques for data analysis, circuit design and construction, as well as probe manufacturing.

Jeremy Buck graduated from Queen's University in 2013 with the B.Sc. in Engineering Physics, and completed a M.ASc. in 2015 as a collaboration between Queen's University and the Royal Military College of Canada. Jeremy is currently working for the Canadian Nuclear Laboratories in Chalk River, ON.

Peter Ross Underhill received the B.Sc. degree in physics and math from Trent University, Peterborough, ON, Canada in 1977, and the D.Phil. degree from York University, York, U.K., in 1981, which he attended as a Commonwealth Scholar. He has 30 years of research and development experience, both in industry and academia, in various aspects of materials research. His most recent work at the Royal Military college of Canada, Kingston, ON, has been in eddy current testing and development of pulsed eddy current systems for applications including inspection of submarine hulls, aircraft components and steam generator tubing.

Jordan E. Morelli (M'01-SM'08) received the B.Eng. degree in Electrical Engineering from the Royal Military College of Canada, Kingston, ON, Canada in 1996; the M.A.Sc. degree in Electrical Engineering from the University of Windsor, Windsor, ON, Canada in 1998; and the Ph.D. degree in Electrical Engineering from the University of Saskatchewan, Saskatoon, SK, Canada in 2003. In 2003 he joined the Department of Physics, Engineering Physics & Astronomy at Queen's University, Kingston, ON, Canada as an Assistant Professor. In 2010 he was promoted to the rank of Associate Professor. His research has been concerned with artificial intelligence based optimization and control especially of magnetically confined plasma, electrical distribution systems, and recently eddy current based non-destructive evaluation.

Thomas W. Krause received the B.Sc. degree in physics from the University of Calgary, AB, Canada, in 1987, and the M.Sc. and Ph.D. degrees in physics from McMaster University, Hamilton, ON, Canada, in 1989 and 1992, respectively. He has 25 years of research and development experience on advanced nondestructive testing technology. His most recent ten years as Professor at the Royal Military College of Canada, Kingston, ON, has involved research in pulsed eddy current, eddy current, magnetic Barkhausen noise and ultrasonics.